Early Disk-Galaxy Formation from JWST to the Milky Way
Proceedings IAU Symposium No. 377, 2024
F. Tabatabaei, B. Barbuy & Y.-S. Ting, eds.
doi:10.1017/S174392132300100X

JWST unveils a population of "red-excess" galaxies in Abell2744 and in the coeval field

Benedetta Vulcani[1] and GLASS team

[1]INAF Osservatorio Astronomico di Padova, vicolo dell'Osservatorio 5, 35122 Padova, Italy.
email: benedetta.vulcani@inaf.it

Abstract. We combine JWST/NIRCam imaging and MUSE data to characterize the properties of galaxies in the cluster Abell2744 ($z = 0.3064$) and in its immediate surroundings. We discover a "red-excess" population in F200W−F444W colors in both the cluster regions and the field. These galaxies have normal F115W-F150W colors and rather blue rest frame B−V colors, but are up to 0.8 mag redder than red sequence galaxies in F200W−F444W. Considering morphology, many cluster galaxies show signatures consistent with ram pressure stripping, while field galaxies have features resembling interactions and mergers. Our hypothesis is that these galaxies are characterized by dust enshrouded star formation: a JWST/NIRSpec spectrum for one of the galaxies is dominated by a strong PAH at $3.3\mu m$, suggestive of dust obscured star formation.

Keywords. Galaxies: formation, Galaxies: evolution, Galaxies: clusters

1. Introduction

Dusty galaxies have been detected throughout cosmic history (e.g. Smail et al. 1997). Their infrared luminosity mainly originates from dust-enshrouded intense episodes of massive star formation (e.g. Yan et al. 2005). Several works have proposed that, at least at $z < 1$, the amount of dust obscuration correlates with the surrounding environment (e.g. Duc et al. 2002 Koyama et al. (2008) suggested that the mid-infrared (MIR) activity is enhanced in 'medium-density' environments such as cluster outskirts. The most likely physical mechanisms at work in these medium-density regions are still debated: Hopkins et al. (2008); Martig & Bournaud (2008) point to galaxy-galaxy interaction or mergers, Jachym et al. (2007); Cen et al. (2014) point to hydrodynamical effects.

Abell 2744 at $z = 0.3064$ (RA = 00:14:20.952, Dec. =−30:23:53.88) is a very massive cluster (virial mass of $7.4 \times 10^{15} M_{\odot}$, Jauzac et al. 2016), it is in a particularly dynamic state due to its merging history and is characterized by distinct components identified using X-ray and optical spectroscopy (Owers et al. 2011). Its host galaxies hence should feel the strongest environmental effects (Boselli & Gavazzi 2006). Peering inside the properties of the cluster members adds significant knowledge on the role of environment in shaping galaxy evolution.

Here we exploit *JWST*/NIRCam observations, combined with VLT/MUSE data, to investigate the properties of a population of galaxies with normal optical and F115W−F150W colors and an excess of up to 0.8 mag in F200W−F444W over the standard red sequence.

2. Data observations and reduction

We use JWST/NIRCam imaging obtained by the GLASS-JWST program ERS-1324 (Treu et al. 2022), the UNCOVER program GO-2561 (Bezanson et al. 2022) and the DDT

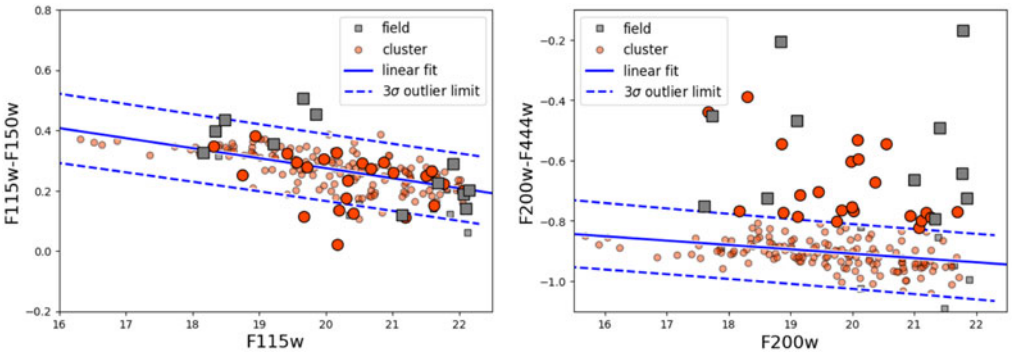

Figure 1. Observed color-magnitude diagram. Left: F115W-F150W vs. F115W. Right: F200W-F444W vs. F200W. Red circles: cluster galaxies; grey squares: field galaxies. The blue solid line represents the best fit of the relation, obtained with an iterative 3σ clipping procedure. The dashed line shows the 3σ error. Galaxies deviating more than 3σ from the best fit in the F200W-F444W vs. F200W plane are indicated with larger symbols in both panels.

Program 2756. Taken together, these surveys provide contiguous coverage in 8 bands from 0.8 to 4.5 μm over 46.5 square arcmin (Paris et al. 2023). Image reduction and calibration, and the methods used to detect sources and measure multi-band photometry in all fields closely follow that of Merlin et al. (2022) and Paris et al. (2023).

We make use of all the available VLT/MUSE spectroscopy in the surrounding of the A2744 cluster. For the cluster central region, we rely on the data from the MUSE Lensing Cluster GTO program (Bacon et al. 2017, Richard et al. 2021). Beyond the cluster central part, we make use of MUSE observations of the GLASS-JWST NIRCam fields obtained through the ESO DDT program 109.24EZ.001 (Prieto et al. 2022).

3. Galaxy sample and galaxy properties

We select galaxies that are both in the MUSE and NIRCam footprints. This choice allows us to assemble a sample with a spectroscopic completeness of 85% at F115W= 22.2 mag. We separate galaxies based on their environment: we define as cluster members galaxies lying within $3\sigma_{cl}$ from the cluster redshift and as field galaxies the non members in the redshift range $0.15 < z < 0.55$. The final cluster sample includes 170 galaxies, the field sample 20. Observed total magnitudes and colors are described by Paris et al. (2023). We obtain rest frame colors, stellar masses and attenuation by fitting synthetic stellar templates to the NIRCam photometry as in Santini et al. (2023).

4. Results and Discussion

We explore a new set of galaxy colors and unveil trends undetected in the optical regime. Figure 1 shows the observed F115W-F150W (left) and F200W-F444W colors (right). The first relation has measured scatter of 0.04 mag. This value is similar to the scatter of color magnitude relation of local clusters (e.g. Valentinuzzi et al. 2011). No clear differences emerge between cluster and field galaxies. Considering instead the F200W and F444W bands, a population of "red-excess" galaxies emerges. Fitting the relation and considering galaxies outside the 3σ (=0.16 mag) region, we find that while only one field galaxy has a color bluer than the fitted relation, 32 galaxies ($\sim 17\%$) have significantly redder colors than the bulk of the population: 11 of them are in the field, 21 in the cluster. Galaxies are up to 0.8mag redder than the best-fit. These galaxies include, but are not limited to, the reddest outliers in the F115W-F150W color. Galaxies with typical F115W-F150W colors can be much redder at longer wavelengths. According to

https://doi.org/10.1017/S174392132300100X Published online by Cambridge University Press

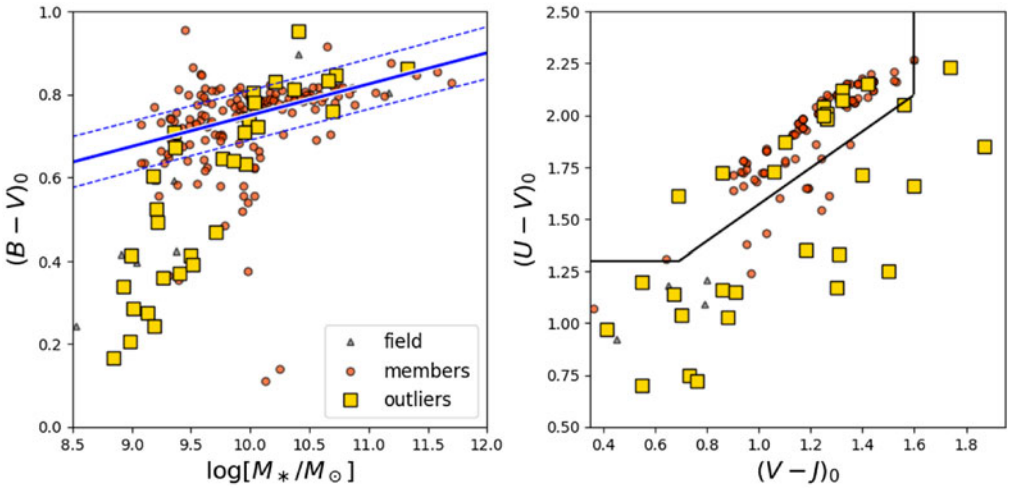

Figure 2. Left: Rest frame B-V vs stellar mass for the cluster members (red circles), field galaxies (grey triangles) and the outliers population (gold squares). The blue line represent the best fit of the red sequence, along with the 3σ scatter. Right: Rest frame U-V vs. V-J diagrams of the outliers, compared to normal field and cluster galaxies.

the UVJ diagram (Fig. 2), 34±8% of the red excess galaxies are passive. They represent 50.0±0.7% of the (cluster+field) star forming population. Most of the red excess are blue at the rest frame optical wavelengths: 20/32 galaxies lie below the red sequence, eleven on the main sequence and only one above (Fig. 2).

We measure various indicators of galaxy morphologies, and find that red excess galaxies have higher values of asymmetry (Pawlik et al. 2016) and M20 (i.e. the ratio of the second order moment of the brightest 20% of pixels and of all pixels in a galaxy's image, Lotz et al. 2004): the median value of asymmetry for the outliers is 0.094±0.009, while for the normal population is 0.075±0.004; a Kolmogorov-Smirnov (KS) test rejects with high confidence (P_{val} =0.002) the hypothesis that samples are drawn from the same parent distribution. The the median value of M20 for the outliers is −1.98±0.02, while for the normal population is −1.90±0.005; the KS test in this case is only marginally significant. Overall, a variety of different morphologies emerges (not shown), from smooth to clumpy light distributions, to well defined spiral arms, to disturbed galaxies. Many galaxies show asymmetries, some of them show signs of unwinding arms, similar to what observed in local cluster galaxies (Vulcani et al. 2022). Fig. 3 shows one example of a red excess galaxy along with the F200W-F444W color map. The red color excess is spread throughout the galaxy disk. Overall, disturbances in morphologies must be due to different physical mechanisms in the different environments, as in the field merger and interactions might be responsible for the observed morphology, while in clusters we can advocate hydrodinamical mechanisms, as ram pressure stripping (Gunn & Gott 1972).

To get further insight on the origin of the observed red colors, we inspect the NIRSpec spectrum for one of the galaxies (Fig. 3), obtained as part of the GLASS-JWST survey. We refer to Morishita et al. (2023) for details of the NIRSpec observations and data reduction. The most prominent feature is the 3.3μm Polycyclic Aromatic Hydrocarbon (PAH) line, which has a rest frame Equivalent Width is of 590±30 Å. The prominence of this line can be responsible of the elevated fluxes measured in F444W. The 3.3μm PAH emission can place constraints on the contribution of dust obscured star formation and active galactic nuclei (AGN) to the cosmic IR background (e.g. Schweitzer et al. 2006). In general, PAH emission features are proposed to be an excellent indicator of star-formation

https://doi.org/10.1017/S174392132300100X Published online by Cambridge University Press

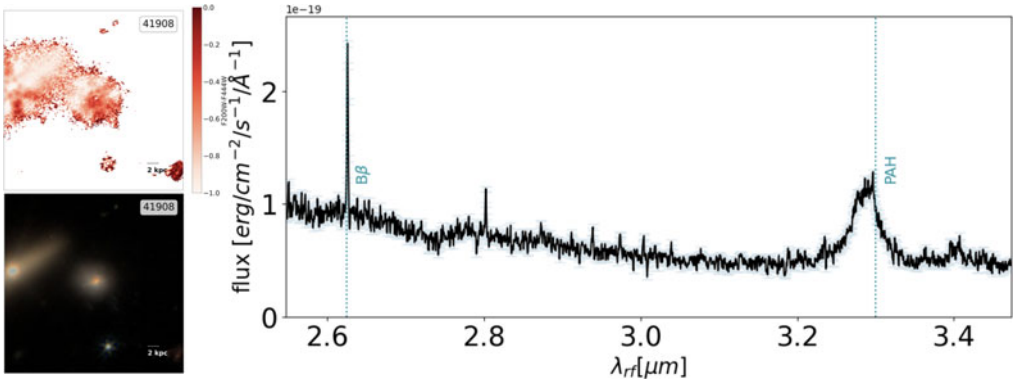

Figure 3. Left: F200W-F444W maps and corresponding color composite (F115W+F150W+F200W) images of one red excess galaxy. The physical scale is reported in the bottom right corners. Right: JWST/NIRSpec spectrum for the same galaxy. The position of the Brackettβ and of the PAH 3.3μm is shown.

activity (e.g., Peeters (2004)). PAHs are illuminated by UV photons, mostly from hot stars in star forming regions (Spoon et al. 2004; Calzetti 2011), while they are destroyed by hard radiation from an AGN central engine (Voit 1992).

We hypothesize that the PAH is due to heavily obscured star formation, similarly to what proposed to explain various populations of galaxies revealed by the Spitzer Space Telescope with significant excesses in their NIR emission, compared to what is expected from an old stellar population, at various redshifts (e.g., Papovich et al. (2007)). A larger sample of galaxies with red colors and NIR spectra will be needed to study in detail the origin of the red excess.

References

Bacon et al. 2017, A&A, 608, 1
Bezanson et al. 2022, arXiv:2212.04026
Boselli & Gavazzi 2006, PASP, 118 517
Calzetti 2011, EASPS, 46, 133
Cen et al. 2014, PNAS, 111 7914
Duc et al. 2002, A&A, 382 60
Gunn & Gott et al. 1972, ApJ, 176 1
Hopkins et al. 2008, pJS, 175 356
Jachym et al. 2007, A&A, 472 5
Jauzac et al. 2016, MNRAS, 463 3876
Koyama et al. 2008, MNRAS, 391 1758
Lotz et al. 2004, ApJ, 672, 177
Martig & Bournaud 2008, MNRAS, 385L 38
Merlin et al. 2022, ApJL, 938, L14
Morishita et al. 2022, arXiv:2211.09097
Morishita, T., Roberts-Borsani, G., Treu, T. et al. 2023, ApJ, 947, L24
Owers et al. 2011, ApJ, 728 270
Papovich et al. 2007, ApJ, 668, 45
Paris et al. 2023, arXiv:2301.0217P
Pawlik et al. 2016, MNRAS 456, 3032
Peeters et al. 2004, ApJ, 613, 986
Prieto-Lyon et al. 2022, arXiv:2211.12548
Richard et al. 2021, A&A, 646, 83
Santini et al. 2023, ApJL, 942, 27

https://doi.org/10.1017/S174392132300100X Published online by Cambridge University Press

Schweitzer et al. 2006, ApJ, 649, 79
Smail et al. 1997, ApJ, 490L 5
Spoon et al. 2004, A&A, 414, 873
Treu et al. 2022, ApJ, 935 110
Valentinuzzi et al. 2011 A&A, 536, 34
Voit 1992, MNRAS,258, 841
Vulcani et al. 2022, ApJ, 927, 91
Yan et al. 2005, ApJ, 628 604

https://doi.org/10.1017/S174392132300100X Published online by Cambridge University Press